Dynamics at a smeared phase transition

2005 J. Phys. A: Math. Gen. 38 2349

(http://iopscience.iop.org/0305-4470/38/11/003)

INSTITUTE OF PHYSICS PUBLISHING JOURNAL OF PHYSICS A: MATHEMATICAL AND GENERAL

J. Phys. A: Math. Gen. **38** (2005) 2349–2358 doi:10.1088/0305-4470/38/11/003

Dynamics at a smeared phase transition

Bernard Fendler[1,2], **Rastko Sknepnek**[1,3] **and Thomas Vojta**[1]

[1] Department of Physics, University of Missouri–Rolla, Rolla, MO 65409, USA
[2] Department of Physics, Florida State University, Tallahassee, FL 32306, USA
[3] Department of Physics and Astronomy, McMaster University, Hamilton, ON L8S 4M1, Canada

Received 29 September 2004, in final form 14 January 2005
Published 2 March 2005
Online at stacks.iop.org/JPhysA/38/2349

Abstract

We investigate the effects of rare regions on the dynamics of Ising magnets with planar defects, i.e., disorder perfectly correlated in two dimensions. In these systems, the magnetic phase transition is smeared because static long-range order can develop on isolated rare regions. We first study an infinite-range model by numerically solving local dynamic mean-field equations. Then we use extremal statistics and scaling arguments to discuss the dynamics beyond mean-field theory. In the tail region of the smeared transition the dynamics is even slower than in a conventional Griffiths phase: the spin autocorrelation function decays like a stretched exponential at intermediate times before approaching the exponentially small equilibrium value following a power law at late times.

PACS numbers: 64.60.Ht, 05.50.+q, 75.10.Nr, 75.40.Gb

1. Introduction

In recent years, the influence of quenched disorder on phase transitions and critical points has reattracted considerable attention. A particularly interesting source of new phenomena are the effects of rare spatial regions which can be locally in the wrong phase. These rare regions or 'Griffiths islands' fluctuate very slowly because flipping them requires changing the order parameter in a large volume. Griffiths [1] showed that this leads to a non-analytic free energy everywhere in an entire temperature region close to the transition, which is now known as the Griffiths phase [2] or the Griffiths region. In generic classical systems with uncorrelated disorder, the contribution of the Griffiths singularities to thermodynamic (equilibrium) observables is very weak since the singularity in the free energy is only an essential one [1, 3]. In contrast, the consequences for the dynamics are much more severe with the rare regions dominating the behaviour for long times. In the Griffiths region, the spin autocorrelation function $C(t)$ decays very slowly with time t, like $\ln C(t) \sim -(\ln t)^{d/(d-1)}$ for Ising systems [2, 4–7], and like $\ln C(t) \sim -t^{1/2}$ for Heisenberg systems [7, 8]. Many of these results have been confirmed by rigorous calculations of disordered Ising models [9–11].

The effects of impurities are greatly enhanced by long-range spatial disorder correlations. In an Ising model with linear defects, the thermodynamic Griffiths singularities are given by power laws with the average susceptibility actually diverging in a finite temperature region. The critical point itself is of exotic infinite-randomness type and displays activated rather than power-law scaling. This was first found in the McCoy–Wu model [12, 13], a disordered 2D Ising model in which the disorder is perfectly correlated in one dimension and uncorrelated in the other. Later it was studied in great detail in the context of the quantum phase transition of the random transverse-field Ising model where the imaginary time dimensions plays the role of the 'correlated' direction [14].

Recently, it has been shown that even stronger effects than these power-law (quantum) Griffiths singularities can occur in Ising models with planar defects [15, 16]. Because the disorder is perfectly correlated in two directions, the effective dimensionality of the rare regions is 2. Therefore, an isolated rare region can undergo the phase transition independently from the bulk system. This leads to a destruction of the global sharp phase transition by smearing. Similar smearing effects have also been found in itinerant quantum magnets [17] and at a non-equilibrium transition in the presence of linear defects [18]. In all of these cases, the effective dimensionality of a rare region is above the lower critical dimension of the problem which allows the rare region to order independently.

In this paper, we investigate the *dynamics* of an Ising model with planar defects in the vicinity of this smeared phase transition. We show that the dynamics in the 'tail' of the smeared transition is even slower than in a conventional Griffiths phase. The autocorrelation function decays like a stretched exponential at intermediate times followed by power-law behaviour at late times. The paper is organized as follows. In section 2, we introduce the model and briefly summarize the results for the thermodynamics of the smeared transition to the extent necessary for the discussion of the dynamics. In section 3, we numerically solve dynamical mean-field equations and compare the results to predictions based on a variational approach. In section 4, we use general scaling arguments in connection with extremal statistics to go beyond mean-field theory. Conclusions are presented in section 5.

2. The model and its thermodynamics

For definiteness we consider a d-dimensional Ising model with bond disorder completely correlated in the $d_C = 2$ directions x_1 and x_2 but uncorrelated in the remaining $d_\perp = d - d_C$ directions $x_3, \ldots, x_d$. Classical Ising spins $S_{\mathbf{x}} = \pm 1$ reside on the sites $\mathbf{x}$ of a hypercubic lattice. They interact via nearest-neighbour interactions. In the clean system all interactions are independent of the lattice site; their values are J_0 for bonds in the uncorrelated directions and $J_0/4$ for bonds in the x_1 and x_2 directions. We have chosen this scaling of the interactions because it leads to mean-field equations compatible with the corresponding thermodynamic mean-field theory [15]. The planar defects are modelled by weakening the bonds in the (x_1, x_2)-planes at random positions in the uncorrelated directions. The system effectively consists of blocks separated by parallel planes of weak bonds. The Hamiltonian of the system is given by

$$H = -\frac{1}{4}\sum_{\mathbf{x}} J(\mathbf{x}_\perp)\left[S_{\mathbf{x}}S_{\mathbf{x}+\mathbf{e}_1} + S_{\mathbf{x}}S_{\mathbf{x}+\mathbf{e}_2}\right] - \sum_{\mathbf{x}}\sum_{j=3}^{d} J_0 S_{\mathbf{x}}S_{\mathbf{x}+\mathbf{e}_j}, \tag{1}$$

where $\mathbf{e}_j$ is a unit vector in the direction x_j, $\mathbf{x}_\perp$ is the projection of $\mathbf{x}$ on the uncorrelated directions $x_3, \ldots, x_d$ and $J(\mathbf{x}_\perp)$ is the random coupling constant in the (x_1, x_2)-planes. The

values of $J(\mathbf{x}_\perp)$ are drawn from a binary distribution

$$J(\mathbf{x}_\perp) = \begin{cases} cJ_0 & \text{with probability } p \\ J_0 & \text{with probability } (1-p) \end{cases} \tag{2}$$

characterized by the concentration p and the relative strength c of the weak bonds ($0 \leqslant p \leqslant 1$, $0 < c \leqslant 1$).

We now briefly summarize the results on the thermodynamics of this system [15, 16] to the extent necessary for the discussion of the dynamics. The clean system ($p = 0$) undergoes a magnetic phase transition at some temperature T_c^0, with the order parameter being the total magnetization

$$m = \frac{1}{V} \sum_{\mathbf{x}} \langle S_{\mathbf{x}} \rangle, \tag{3}$$

where V is the system volume and $\langle \cdots \rangle$ is the thermodynamic average. In the disordered system ($p > 0$), a crucial role is played by rare strong disorder fluctuations: there is a small but non-zero probability for finding large spatial regions in the $\mathbf{x}_\perp$ direction devoid of any impurities. These regions can be locally in the ordered phase even if the bulk system is in the disordered phase. Because of the disorder correlations, these rare regions are infinite in the x_1 and x_2 directions but finite in the remaining directions. Thus, each rare region is equivalent to a two-dimensional Ising system and can undergo a real phase transition *independently* of the rest of the system. The resulting effect is much stronger than the conventional Griffiths effects [1, 2]: the global phase transition is destroyed by smearing [15]; and the order parameter develops very inhomogeneously in space with different parts of the system (i.e., different $\mathbf{x}_\perp$ regions) ordering independently at different temperatures. Correspondingly, the correlation length in the $\mathbf{x}_\perp$ direction remains finite for all temperatures.

Using extremal statistics, the leading thermodynamic behaviour can be easily worked out in the 'tail' of the smeared transition, i.e., in the parameter region where a few islands have developed static order but their density is so small that they can be treated as independent. The probability w of finding a large region of linear size L_R (in $\mathbf{x}_\perp$-space) devoid of any impurities is, up to pre-exponential factors, given by

$$w \sim (1-p)^{L_R^{d_\perp}} = \exp\left[L_R^{d_\perp} \ln(1-p)\right]. \tag{4}$$

As discussed above, such a rare region develops static long-range (ferromagnetic) order at some temperature $T_c(L_R)$ below the clean bulk critical temperature T_c^0. The value of $T_c(L_R)$ varies with the size of the rare region; the largest islands will develop long-rage order closest to the clean critical point. According to finite-size scaling we obtain

$$T_c(L) - T_c^0 = r_c(L_R) = -AL_R^{-\phi}, \tag{5}$$

where ϕ is the finite-size scaling shift exponent of the clean system and A is the amplitude for the crossover from d dimensions to a slab geometry infinite in two dimensions but finite in $d_\perp = d - 2$ dimensions. The reduced temperature $r = T - T_c^0$ measures the distance from the *clean* critical point. If hyperscaling is valid, the finite-size shift exponent fulfils $\phi = 1/\nu$. Combining (4) and (5) we obtain the probability for finding a rare region that becomes critical at r_c as

$$w(r_c) \sim \exp(-B|r_c|^{-d_\perp/\phi}) \qquad (\text{for } r_c \to 0-) \tag{6}$$

where the constant B is given by $B = -\log(1-p)A^{d_\perp/\phi}$. The total (or average) order parameter m is obtained by integrating over all rare regions which are ordered at r, i.e., all rare regions having $r_c > r$. Since the functional dependence on r of the order parameter on

a given island is of power-law type, it does not enter the leading exponentials but only the pre-exponential factors. To exponential accuracy, we therefore obtain

$$m \sim \exp(-B|r|^{-d_\perp/\phi}) \qquad (\text{for } r \to 0-). \tag{7}$$

Thus, the total magnetization develops an exponential tail towards the disordered phase which reaches all the way to clean critical point. Analogous estimates show that the homogeneous magnetic susceptibility does not diverge anywhere in the tail region of the smeared transition because the exponentially decreasing island density overcomes the power-law divergence of the susceptibility of an individual island. However, there is an essential singularity at the clean critical point produced by the vanishing density of ordered islands.

3. Local dynamic mean-field approach

We now turn to the main topic of this paper, namely, the dynamic behaviour in the vicinity of the smeared phase transition. We consider a purely relaxational local dynamics without any conservation laws, i.e., model A in the Hohenberg–Halperin classification [19]. Microscopically, it can be realized, e.g., by the Glauber algorithm [20].

In this section, we study the dynamics of the Ising model (1) by numerically solving local dynamic mean-field equations. For definiteness, we consider $d = 3$ spatial dimensions, i.e., $d_\perp = 1$ and $d_C = 2$. A local dynamic mean-field theory of the Hamiltonian (1) can be derived, e.g., by following [21]. The plane magnetizations

$$m_{x_3} = \frac{1}{L_C^2} \sum_{x_1,x_2} S_{\mathbf{x}}, \tag{8}$$

where L_C is the system size in correlated direction, then fulfil the local mean-field equations of motion

$$\frac{1}{\alpha}\frac{\mathrm{d}}{\mathrm{d}t} m_x = -m_x + \tanh\left[(J_0 m_{x-1} + J(x) m_x + J_0 m_{x+1})/T\right]. \tag{9}$$

Here, α is a microscopic relaxation rate which determines the overall time scale. Alternatively, the same equations can be obtained without further approximation from the infinite-range Hamiltonian used in the thermodynamic mean-field theory [15].

Note that the local mean-field equations contain the full spatial dependence of the magnetization on the uncorrelated dimension. In contrast to a global mean-field theory these local equations are therefore capable of describing rare region physics. The stationary solution of (9) corresponds to the thermodynamic local mean-field theory studied in [15]. The clean model ($p = 0$) undergoes a magnetic phase transition at $T_c^0 = 3J_0$, displaying mean-field critical behaviour. Below T_c^0, the diluted system ($p > 0$) develops an exponential magnetization tail of the form $m \sim \exp\left(-B\left|T_c^0 - T\right|^{-1/2}\right)$ following the prediction (7) with $d_\perp = 1$ and $\phi = 2$.

To study the dynamics, we have numerically integrated equations (9) for $\alpha = 1$, $J_0 = 1$, $c = 0.2$, dilutions of $p = 0.2, 0.3, 0.4, 0.5, 0.6, 0.7$ and 0.8 and system sizes (uncorrelated direction) up to $L_\perp = 10^6$ averaging over up to 25 disorder realizations. Let us first analyse the behaviour at the clean critical temperature $T_c^0 = 3.0$ (at the threshold of rare region ordering). The left panel of figure 1 shows the time evolution of the total magnetization $m = (1/L_\perp)\sum_x m_x$ at $T_c^0 = 3$ for several dilutions. The figure shows that the long-time decay of the magnetization is governed by a stretched exponential of the form $\ln m(t) = -Et^{-1/3}$. The decay constant E increases with increasing dilution. The right panel of figure 1 shows E as a function of the dilution p. Clearly, the decay constant depends linearly on $[-\ln(1-p)]^{2/3}$.

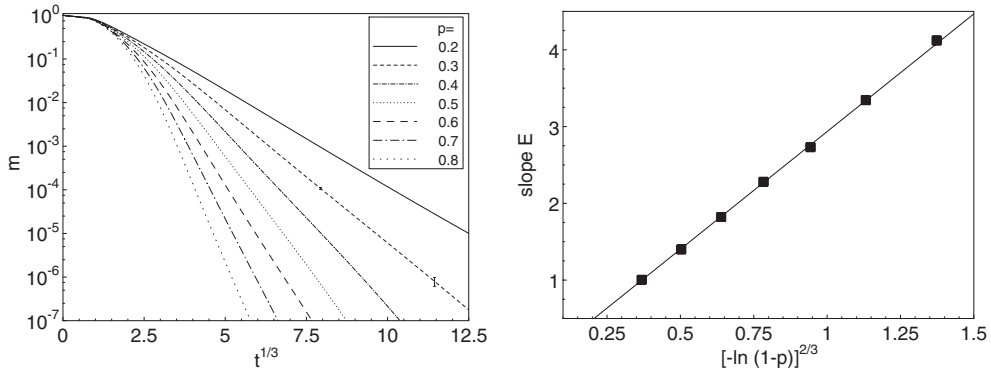

Figure 1. Left: time evolution of the magnetization at the clean critical temperature $T_c^0 = 3$ for several impurity concentrations p starting from a fully polarized state at $t_0 = 0$ to $t_{\max} = 2000$. Parameters are $L_\perp = 10^5$, $J_0 = 1$, $c = 0.2$. The data represent averages of 25 disorder configurations. The long-time behaviour of m follows $\ln m(t) \sim -Et^{-1/3}$. Error bars representing the standard deviation of m are shown for $p = 0.3$. Right: decay constant E of the stretched exponential decay of the magnetization as a function of the impurity concentration p. The solid line is a linear fit to $[-\ln(1-p)]^{2/3}$.

This behaviour can be understood using variational arguments similar to that of Bray [6, 7] for conventional Griffiths effects. At the clean critical point, the correlation time ξ_t of an impurity-free island depends on its linear size L_R via a power law $\xi_t \sim L_R^z$. Here, z is the clean dynamical exponent whose value is 2 for our infinite-range model. The rare region contribution to the time-dependent magnetization $m(t)$ can be obtained by summing over the exponential time dependences of the individual islands with L_R-dependent correlation time. Using (4) we obtain to leading exponential accuracy

$$m(t) \sim \int \mathrm{d}L_R \exp\left[L_R \ln(1-p) - t/\xi_t(L_R)\right]. \tag{10}$$

This integral can easily be evaluated variationally, i.e., within the saddle-point method. The main contribution to m at time t comes from islands of size $L_R^{\mathrm{SP}}(t) \sim [t/(-\ln(1-p))]^{1/3}$. The leading long-time decay of the magnetization at the clean critical point is then given by a stretched exponential

$$\ln m(t) \sim -t^{1/3}[-\ln(1-p)]^{2/3} \tag{11}$$

in complete agreement with the simulation results presented in figure 1.

Before we continue, let us briefly comment on error bars and finite-size effects. A detailed analysis of finite-size effects in our model was performed for the thermodynamics in [15]. A finite-size sample contains only a finite number of islands of a certain size L_R. As long as the number of relevant islands of size L_R^{SP} is large, finite-size effects on the time evolution, figure 1, are small and governed by the central-limit theorem. With increasing time, L_R^{SP} increases and the number of islands of this size decreases. When it becomes of order 1, strong sample-to-sample fluctuations are expected. Finally, when L_R^{SP} becomes larger than the largest island on the sample, the time evolution will cross over from stretched exponential (11) to simple exponential decay. The data in figure 1 show that finite-size effects do not play a significant role in the parameter range shown. Sample-to-sample fluctuations (as represented by the standard deviation of the magnetization) remain small down to $m = 10^{-6}$. Also, no deviations from stretched exponential decay are observed even at the smallest magnetizations shown (they do start to occur below $m \approx 10^{-8}$, though).

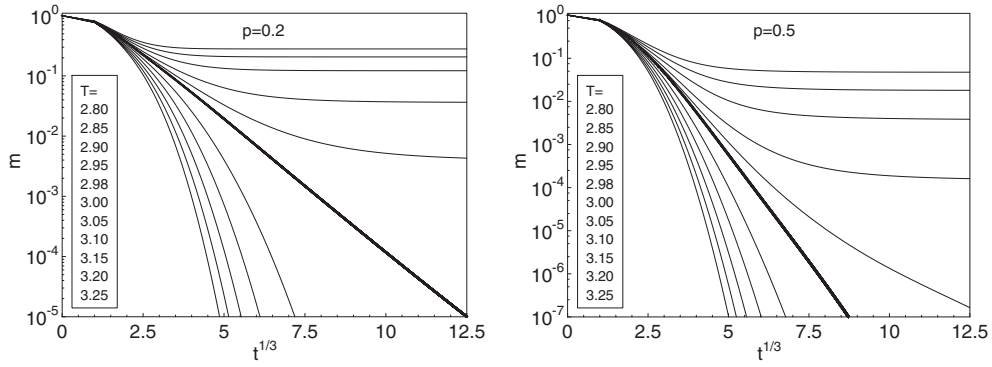

Figure 2. Time evolution of the magnetization at several temperatures from $T = 2.8$ to 3.25 (top to bottom) starting from a fully polarized state at $t_0 = 0$ to $t_{\max} = 2000$. Parameters are as in figure 1. The data represent averages of 25 disorder configurations. The impurity concentrations are $p = 0.2$ (left panel) and $p = 0.5$ (right panel).

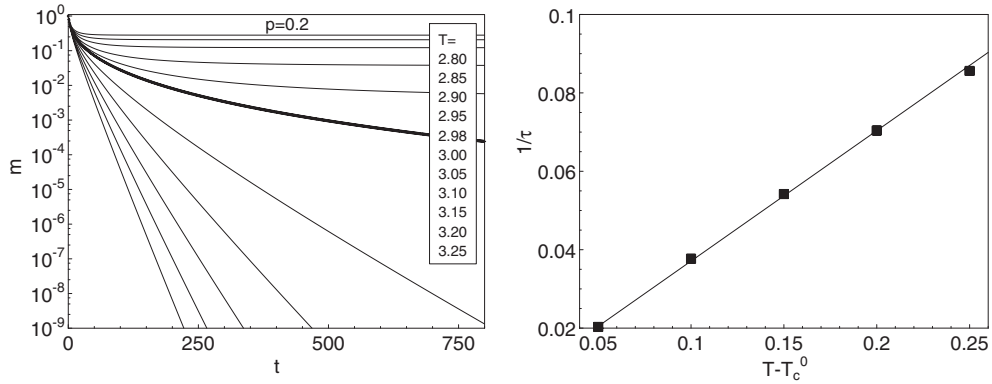

Figure 3. Left: replot of the the $p = 0.2$ data from figure 2. Right: inverse decay time $1/\tau$ as a function of $T - T_c^0$ for the curves above T_c^0.

We now turn to the dynamic behaviour for temperatures close to but not at the clean critical temperature T_c^0. Figure 2 shows the time evolution of the magnetization for several temperatures from $T = 2.8$ to 3.25. At early times, all curves follow the stretched exponential found at T_c^0. After reaching a (temperature-dependent) crossover time t_x, the behaviour qualitatively changes. For temperatures above the clean critical temperature, the magnetization decays faster than the stretched exponential. In fact, the asymptotic decay is exponential $\ln m \sim t/\tau(T)$, as can be seen from a log-linear replot of the $p = 0.2$ data in the left panel of figure 3. The dependence of relaxation time $\tau(T)$ on the temperature T is shown in the right panel of figure 3. Clearly, $1/\tau$ varies linearly with $T - T_c^0$ in good approximation. This behaviour can be understood as follows. For $T > T_c^0$ the correlation time of the largest islands does not diverge, but it is cut off by the distance from the clean critical point, $\xi_t \sim \left(T - T_c^0\right)^{-z\nu}$. For our infinite-range model, $z\nu = 1$. The large islands with this correlation time dominate the variational integral (10) for $m(t)$. This leads to a simple exponential decay with an inverse decay time that depends linearly on $T - T_c^0$.

The more interesting cases are temperatures below the clean critical temperature T_c^0, i.e., the tail region of the smeared transition. Here, the total magnetization approaches an

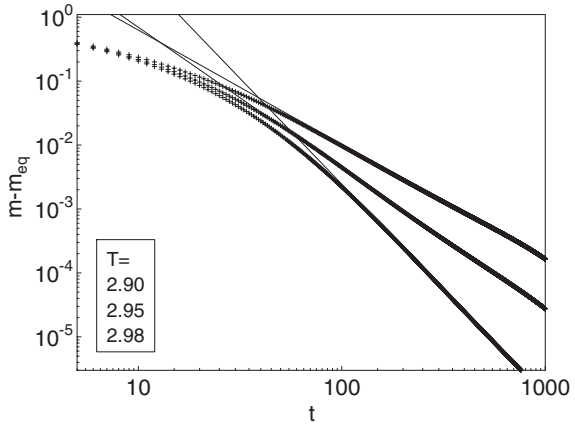

Figure 4. Double-logarithmic plot of the approach of the magnetization to the equilibrium value in the tail of the smeared transition for $T = 2.90$, 2.95 and 2.98 (top to bottom). The impurity concentration is $p = 0.5$; the other parameters are as in figure 1. The straight lines are fits to power laws yielding exponents of 1.78, 2.20 and 3.31, respectively.

exponentially small but non-zero value in the long-time limit, in agreement with (7) and [15]. The approach to this stationary value is very slow. Figure 4 shows $m(t) - m(\infty)$ versus t for $p = 0.5$ and three different temperatures. The data show that the asymptotic decay is governed by a power law with a non-universal, temperature-dependent exponent. To understand this, we note that below T_c^0 the island correlation time has a divergence of the form $\xi_t(T, L_R) \sim \left|T_c^0 - T - AL_R^{-2}\right|^{-1}$. If this is inserted into the variational integral (10), the main contribution comes from (finite-size) islands with $L_R^{-2} \approx \left(T_c^0 - T\right)/A$ because they have diverging correlation time. Carrying out the integral leads to a power law for $m(t) - m(\infty)$.

The distribution of island sizes leads to a corresponding distribution of local correlation times $\xi_t(x)$. Within our infinite-range model, they can be determined by analysing the time evolution of the local magnetization via $\ln m_x \sim -t/\xi_t(x)$. Figure 5 shows the resulting probability distribution $P(\xi_t)$ of the local correlation times at the clean critical point T_c^0 for $p = 0.3$ as determined from ten samples of $L_\perp = 10^6$ sites. The behaviour of the large-ξ_t tail of the probability distribution follows from combining equation (4) with $\xi_t \sim L^2$ leading to $\ln P \sim \xi_t^{-1/2}$.

4. Dynamics from general scaling arguments

In this section, we use general scaling arguments to determine the dynamical behaviour at the smeared transition of our disordered magnet (1) beyond mean-field theory. The interesting physics in the tail of the smeared transition is local because the islands are effectively decoupled from each other, and the spatial correlation length remains finite. An appropriate quantity to study the rare region dynamics is therefore the spin autocorrelation function

$$C(t) = \frac{1}{V}\sum_{\mathbf{x}} \langle S_{\mathbf{x}}(t) S_{\mathbf{x}}(0)\rangle. \tag{12}$$

To determine the leading behaviour of $C(t)$ in the tail of the smeared transition we generalize the variational extremal statistics calculation from section 3 to the non-mean-field case.

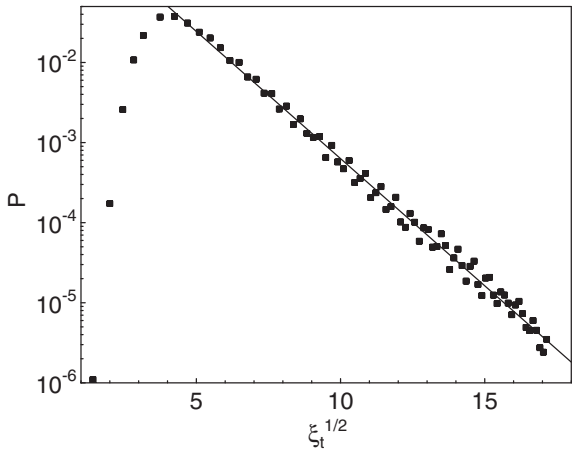

Figure 5. Probability distribution of the local relaxation times at T_c^0 for $p = 0.3$, determined from ten samples of size $L_\perp = 10^6$. The other parameters are as in figure 1. The solid line is a fit of the large-ξ_t tail to $\ln P \sim \xi_t^{-1/2}$.

According to finite-size scaling [22], the behaviour of the correlation time ξ_t of a single rare region of size L_R in the vicinity of the clean bulk critical point can be modelled by (for $T < T_c^0$, i.e., $r < 0$)

$$\xi_t(r, L_R) \sim L_R^{(z\nu - \tilde{z}\tilde{\nu})/\nu} \left| r + A L_R^{-1/\nu} \right|^{-\tilde{z}\tilde{\nu}}. \tag{13}$$

Here, ν and z are the correlation length and dynamical exponents of a d-dimensional system, respectively, and $\tilde{\nu}$ and $\tilde{z}$ are the corresponding exponents of a d_C-dimensional system.

Let us first consider the time evolution of the autocorrelation function $C(t)$ at the clean critical point T_c^0. For $r = 0$, the correlation time (13) simplifies to $\xi_t \sim L_R^z$. Similar to the total magnetization in the mean-field treatment above, the rare region contribution to $C(t)$ is obtained by simply summing over the exponential time dependences of the individual islands with L_R-dependent correlation time. Using (4) we obtain to exponential accuracy

$$C(t) \sim \int \mathrm{d}L_R \exp\left(L_R^{d_\perp} \ln(1-p) - Dt \big/ L_R^z \right) \tag{14}$$

where D is a constant. This integral can easily be evaluated within the saddle-point method. The leading long-time decay of the autocorrelation function $C(t)$ at the clean critical point is given by a stretched exponential

$$\ln C(t) \sim -[-\ln(1-p)]^{z/(d_\perp + z)} t^{d_\perp/(d_\perp + z)}. \tag{15}$$

For $T > T_c^0$, i.e., $r > 0$, the correlation time does not diverge for any L_R. Instead, the correlation time of the large islands saturates at $\xi_t(r, L_R) \sim r^{-z\nu}$ for $L_R > (r/A')^{-\nu}$. The autocorrelation function $C(t)$ can again be evaluated as an integral over all island contributions. For intermediate times $t < t_x \sim |r|^{-(d_\perp + z)\nu}$, the autocorrelation function follows the stretched exponential (15). For times larger than the crossover time t_x, we obtain a simple exponential decay $\ln C(t) \sim -t/\tau$ with the decay time $\tau \sim r^{-z\nu}$. Our results for $T \geqslant T_c^0$ agree with those for conventional Griffiths effects [7]. This is not surprising, because above T_c^0, there is no difference between the Griffiths and the smearing scenarios: in both cases, all rare regions are locally still in the disordered phase.

This changes below the clean critical point T_c^0. For $r < 0$, we repeat the saddle-point analysis with the full expression (13) for the correlation length. Again, for intermediate times

$t < t_x$, the decay of the average density is given by the stretched exponential (15). For times larger than the crossover time t_x the system realizes that some of the rare regions have developed static order and contribute to a non-zero equilibrium value of the autocorrelation function $C(t)$. The approach of $C(t)$ to this equilibrium value is dominated by finite-size islands with $L_R \sim (-r/A)^{-\nu}$ because they have diverging correlation time. As a result, we obtain a power law

$$C(t) - C(\infty) \sim t^{-\psi}. \tag{16}$$

The value of ψ cannot be found by our methods since it depends on the neglected pre-exponential factors.

The behaviour of the *local* autocorrelation function $C(\mathbf{x}, t) = \langle S_{\mathbf{x}}(t) S_{\mathbf{x}}(0) \rangle$ is spatially inhomogeneous because the local correlation time depends on the size of the underlying rare region. The probability distribution $P(\xi_t)$ of these of local (island) relaxation times can be obtained from (4) and (13). At the clean critical point T_c^0 we find

$$P(\xi_t) \sim \exp\left(-D\,[-\ln(1-p)]\,\xi_t^{d_\perp/z}\right), \tag{17}$$

where D is a constant.

5. Conclusions

To summarize, we have studied the dynamic behaviour of Ising magnets with planar defects. In these systems the magnetic phase transition is smeared because rare strongly coupled spatial regions independently undergo the phase transition. In the rare-region dominated tail of the smeared transition, the dynamics is very slow. Using general scaling arguments, we have shown that the spin autocorrelation function decays in two stages, a stretched exponential decay at intermediate times followed by a power-law approach to the exponentially small stationary (equilibrium) value. We have illustrated these general scaling results by computer simulations of an infinite-range model.

Let us briefly compare our results to the dynamics in a conventional Griffiths phase (as produced by uncorrelated disorder) [2, 4–7]. In both cases, rare regions dominate the long-time dynamics. In a conventional Griffiths phase, the finite-size rare regions remain fluctuating for all temperatures above the dirty critical point, i.e., their island correlation times *remain finite*. As a result, the autocorrelation function decays like $\ln C(t) \sim -(\ln t)^{d/(d-1)}$ for Ising systems [2, 4–7], and $\ln C(t) \sim -t^{1/2}$ for Heisenberg systems [7, 8]. In contrast, in the tail of a *smeared* transition, the effects of the rare regions are even stronger because individual islands can undergo the phase transition independently, connected with a *divergent* island correlation time. This leads to an even slower power-law decay of the spin autocorrelation function as shown in section 4.

We emphasize that we have considered a purely relaxational (local) dynamics corresponding to model A in the Hohenberg–Halperin classification [19]. Other dynamic algorithms require separate investigations. For instance, model B dynamics globally conserves the order parameter. In this context, an interesting question is: How does the interplay of the *local* thermodynamics of the rare regions and the *global* conservation law modify the dynamic behaviour in the tail of the seared transition?

Finally, we note that while the results here have been derived for an Ising model with planar defects, we expect analogous results for other disorder-smeared phase transitions. Indeed, in the tail of the smeared non-equilibrium phase transition of a contact process with extended impurities, a power-law decay of the density was recently found [18].

Acknowledgments

We acknowledge support from the University of Missouri Research Board and from the NSF under grants No DMR-0339147 and PHY99-07949. Parts of this work have been performed at the Aspen Center for Physics and the Kavli Institute for Theoretical Physics.

References

[1] Griffiths R B 1969 *Phys. Rev. Lett.* **23** 17
[2] Randeria M, Sethna J and Palmer R G 1985 *Phys. Rev. Lett.* **54** 1321
[3] Bray A J and Huifang D 1989 *Phys. Rev.* B **40** 6980
[4] Dhar D 1983 *Stochastic Processes: Formalism and Applications* ed D S Argawal and S Dattagupta (Berlin: Springer)
[5] Dhar D, Randeria M and Sethna J P 1988 *Europhys. Lett.* **5** 485
[6] Bray A J and Rodgers G J 1988 *Phys. Rev.* B **38** 9252
[7] Bray A J 1988 *Phys. Rev. Lett.* **60** 720
[8] Bray A J 1987 *Phys. Rev. Lett.* **59** 586
[9] Dreyfus H von, Klein A and Perez J F 1995 *Commun. Math. Phys.* **170** 21
[10] Gielis G and Maes C 1995 *J. Stat. Phys.* **81** 829
[11] Cesi S, Maes C and Martinelli F 1997 *Commun. Math. Phys.* **189** 135
Cesi S, Maes C and Martinelli F 1997 *Commun. Math. Phys.* **189** 323
[12] McCoy B M and Wu T T 1968 *Phys. Rev.* **176** 631
McCoy B M and Wu T T 1969 *Phys. Rev.* **188** 982
[13] McCoy B M 1969 *Phys. Rev. Lett.* **23** 383
[14] Fisher D S 1992 *Phys. Rev. Lett.* **69** 534
Fisher D S 1995 *Phys. Rev.* B **51** 6411
[15] Vojta T 2003 *J. Phys. A: Math. Gen.* **36** 10921
[16] Sknepnek R and Vojta T 2004 *Phys. Rev.* B **69** 174410
[17] Vojta T 2003 *Phys. Rev. Lett.* **90** 107202
[18] Vojta T 2004 *Phys. Rev.* E **70** 026108
Dickison M and Vojta T 2005 *J. Phys. A: Math. Gen.* **38** 1199
[19] Hohenberg P C and Halperin B I 1977 *Rev. Mod. Phys.* **49** 435
[20] Glauber R J 1963 *J. Math. Phys.* **4** 294
[21] Stanley H E 1987 *Introduction to Phase Transitions and Critical Phenomena* (Oxford: Oxford University Press)
[22] Barber M N 1983 *Phase Transitions and Critical Phenomena* ed C Domb and J L Lebowitz (London: Academic)